4.0 Sediment Transport Model Parameter Fitting

4.1 Introduction

Gerrard (1991) noted that materials on hillslopes can be moved by a number of mechanisms including; rainsplash, surface wash, solution and mass movement. The processes of solution and mass movement are not of relevance to the current study, however rainsplash and surface wash erosion were observed on the field plot. Suspended and bedload sediment data collected from observed storm events enabled the parameterisation of a number of models that can be used to predict rates of erosion.

The potential effect of fluvial erosion of the above-ground landform on the surrounding environment of Magela Creek, was reported in Section 1.0, and emphasises the importance of erosion rate prediction.

Willgoose and Loch (1996) noted that considerable research had occurred in the Tin Camp Creek area and that the processing of this data would be cost effective. Moliere *et al* (1996) focused upon the two field sites from Tin Camp Creek research, termed the Mica and Quartz sites. The Tin Camp Creek site was chosen in a desktop study by Uren (1992; cited in Moliere *et al*, 1996), as having chemical and physical soil properties that most likely reflected the rehabilitated structure at ERARM after long term weathering.

The ability to quantifiably reduce the erosion rate over time, from the parameterisation of erosion models from data collected from these three studies, will enable more accurate estimation by SIBERIA of the structural state of the rehabilitated landform in the long term.

4.2 Sediment Transportation Models

Willgoose and Riley (1993) described the overland flow erosion model (Equation 4.2.1), as one which is in common use by soil scientists and geomorphologists.

$$\boxed{Q_s = \beta_1 W^{(1-m_1)} Q^{m_1} S^{n_1}} \qquad (4.2.1)$$

where

Q_s = Sediment discharge, (g/s),

Q = Discharge, (L/s),

S = Local slope, (m/m), and

W = Width of hillslope, (m).

Willgoose and Riley continued that the parameters, β_1, m_1 and n_1 are fixed by flow geometry and erosion physics.

Equation (4.2.1) is one of the erosion models that is utilised in this study and has been used in previous work on the Northern Waste Rock Dump (Willgoose and Riley, 1993; and Saynor *et al*, 1995), and in the Tin Camp Creek area (Moliere *et al* ,1996).

The width of hillslope referred to in Equation (4.2.1), 'W', (m), for the current study, is the width of the field plot which was 20 metres. The sediment discharge, 'Q_s', (g/s), is a function of discharge, 'Q',(L), and the suspended sediment concentration 'C',(g/L), (Equation 4.2.2).

$$\boxed{Q_s = Q\,C} \qquad (4.2.2)$$

where

C = Suspended sediment concentration, (g/L).

The overland flow erosion model is parameterised utilising only the suspended sediment concentration data.

The rearrangement of the overland flow erosion model (Equation 4.2.1), gives the total sediment loss model for an entire rainfall event which has also been utilised in previous studies on the Northern Waste Rock Dump and in the Tin Camp Creek area.

The total sediment loss, 'T',(g), over an entire rainfall event, Equation (4.2.3), is based on the work of Evans et al, (1995).

$$\boxed{T = \beta_1 W^{(1 - m_1)} S^{n_1} \int Q^{m_1} dt} \qquad (4.2.3)$$

where

T = Total sediment loss, (g), and

$\int Q^{m_1} dt$ = Function of cumulative runoff over event duration, (L^{m1})

The total sediment loss 'T',(g), (Equation 4.2.3), comprises both suspended and bedload sediment. The differences between the data sets utilised in the overland flow erosion model and the total sediment loss model, enables a comparison between the magnitudes of the parameters β_1 and m_1.

4.3 Data

Complete sets of bedload and suspended sediment data were collected from eight storm events over the 96/97 wet season (Appendix 4.A). Table 4.3.1 lists the date of the occurrence of these storm events and their respective rainfall and runoff characteristics.

Table 4.3.1: Storm events and respective rainfall and runoff characteristics for eight monitored storm events from the natural site.

Storm Event.	*Total Rainfall, (mm).*	*Peak Discharge, (L/s).*
1197	70.2	11.00
12197	5.0[a]	0.25
12197pm	16.5[a]	0.55
17197	29.6	0.35
211971st	11.8	0.40
211972nd	22.4	1.70
23197	43.8	12.00
28197	28.2	2.50

[a] Electronic raingauge failure.

The suspended sediment samples were collected in 600mL Bunzl flasks and processed as described in Appendix 4.A.

Suspended sediment concentrations were plotted against time for all storm events listed in Table 4.3.1, and are featured in Appendix 4.A. Figure 4.3.1 illustrates the suspended sediment concentration, (g/L), plot against time, (hours) for the storm event occurring on the 1st January.

It can be observed from Figure 4.3.1, that the sediograph plotted has a sharp initial incline, two peaks, which are similar to that observed with the hydrograph, and a gradual but considerably fluctuating decline.

All the suspended sediment samples from the eight storm events listed in Table 4.3.1 were utilised to parameterise the overland flow erosion model (Equation 4.2.1).

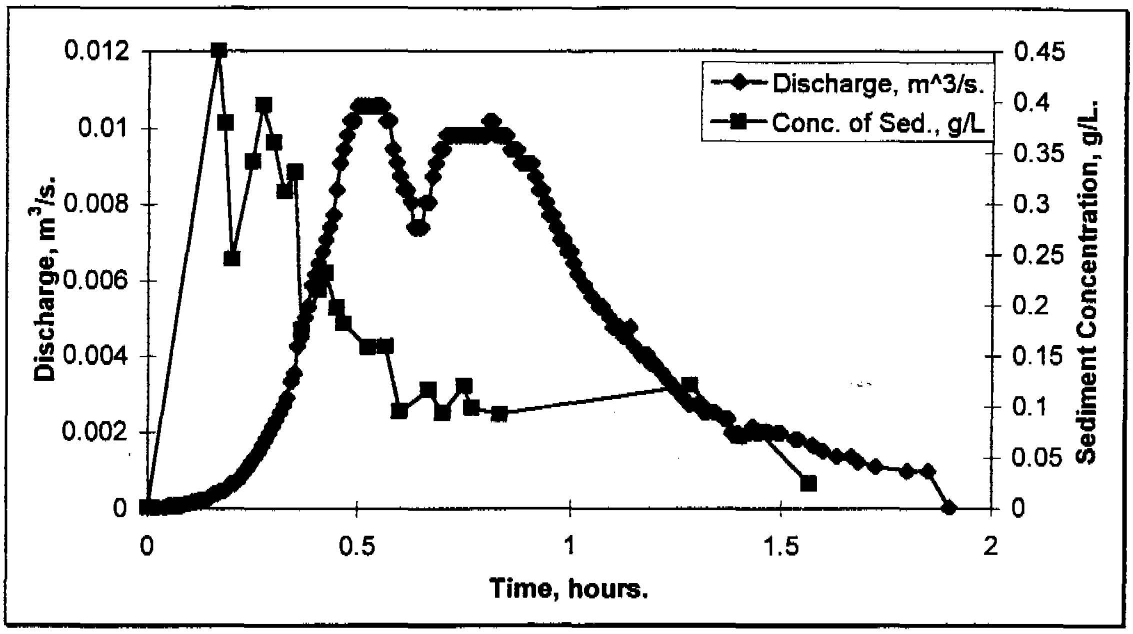

Figure 4.3.1: Plot of the suspended sediment concentration, (g/L), and discharge, (m^3/s) , versus time, (hours), for a storm event occurring on the 1st January 1997.

The overland flow erosion model, Equation (4.2.1), was simplified as Equation (4.3.1).

$$\boxed{Q_s = \beta_1 w^{(1-m_1)} Q^{m_1} S^{n_1}} \qquad (4.2.1)$$

$$\boxed{Q_s = K\,Q^{m_1}} \qquad (4.3.1)$$

where

$$K = \beta_1 w^{(1-m_1)} S^{n_1}$$

A logarithmic transformation of Equation (4.3.1), was performed (Equation 4.3.2).

$$\boxed{\log_{10}(Q_s) = \log_{10}(K) + m_1 \log_{10}(Q)} \qquad (4.3.2)$$

Equation (4.3.2) was fitted with sediment discharge data from all monitored storm events, and is illustrated in Figure 4.3.2.

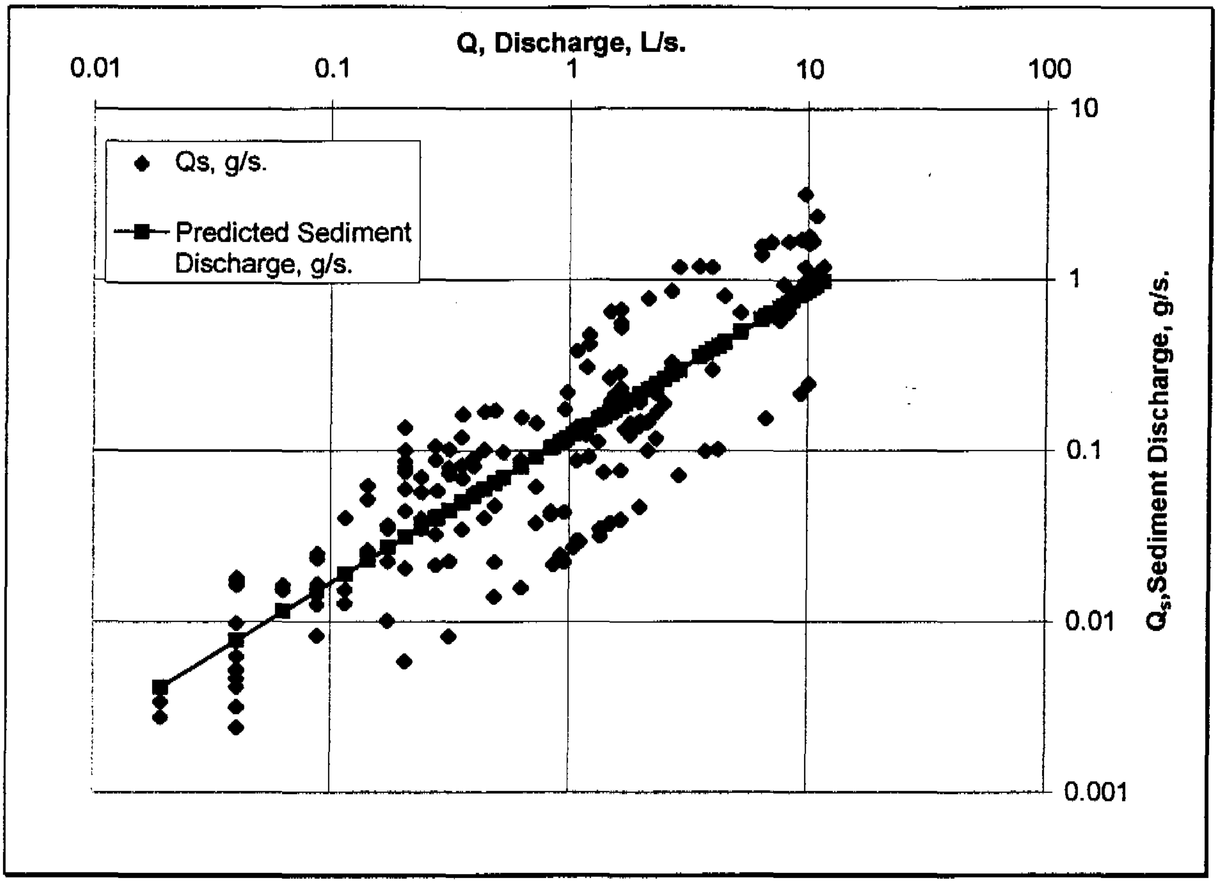

Figure 4.3.2: A log-log regression analysis of 'Q', discharge, (L/s), versus 'Q_s', sediment discharge, (g/s), Equation (4.3.2), was performed utilising all the suspended sediment samples from eight storm events (Table 4.3.1).

The slope of the field plot, determined from a topographic survey reported in Section 3.3, was an average of 0.027 (m/m). The exponent on the slope term of Equation (4.2.1), 'n_l', was assumed to equal 0.69, from previous work, Willgoose and Riley (1993) and Evans *et al* (1995).

Evans *et al* (1995) noted that the parameter 'n_l', originated from Equation (4.3.3).

$$\boxed{Q_s \propto \frac{1}{(d_{50})^{1.5}}} \qquad (4.3.3)$$

where

d_{50} = Median sediment grain diameter, (mm).

Evans *et al* continued that this relationship was derived from the Brown function, Einsteins bed-load function, and Shields formula for bedload. The relationship developed by Evans *et al* (1995), involving the d_{50} values for the cap and batter sites (0.54 and 1.39 mm respectively), yielded a 'n_1' value of 0.71, which was similar to that derived by Willgoose and Riley (1993). A random number of particle size samples where collected and processed from the natural site (Appendix 4.B).The d_{50} for the natural site was determined to be approximately 0.8 mm, (Smith, 1997), which is comparable to that reported for the cap and batter sites.

Equation (4.3.4) highlights the parameter values obtained from the fitting of the overland flow erosion model (Figure 4.3.2).

$$\boxed{Q_s = 0.917\, W^{(1-0.854)} Q^{0.854}\, S^{0.69}} \quad (r^2=0.74, df=169, p<0.001) \qquad (4.3.4)$$

The parameters β_1 and m_1, have mean and standard errors of 0.917 +/- 0.03, and 0.854 +/- 0.04, respectively. The raw output from the regression analysis is listed in Appendix 4.C.

The determination of the total quantity of bedload sediment is an integral component of the total sediment loss model, Equation (4.2.3). The bedload sediment samples collected were processed following the procedure listed in Appendix 4.A.

The total sediment loss model (Equation 4.2.3), was simplified (Equation 4.3.5).

$$\boxed{T = \beta_1 W^{(1-m_1)} S^{n_1} \int Q^{m_1}\, dt} \qquad (4.2.3)$$

$$\boxed{T = K \int Q^{m_1} \, dt} \qquad (4.3.5)$$

where

$$K = \beta_1 W^{(1-m_1)} S^{n_1}$$

Equation (4.3.5) was transformed with logarithms into Equation (4.3.6).

$$\boxed{\log_{10}(T) = \log_{10}(K) + x \log_{10}\left(\int Q^{m_1} \, dt\right)} \qquad (4.3.6)$$

where

x = Transformation parameter.

An initial 'm_1' value was selected and through a trial and error procedure and regression analysis, the magnitude of the parameter 'x' was iterated to unity. The values of the parameters β_1 and m_1, that were associated with the magnitude of the parameter 'x' being equal to 1, were chosen as the fitted parameter values.

The integration of 'Q^{m_1}' with respect to time, from the total sediment loss model (Equation 4.2.3), for a entire rainfall event was determined using a backward difference numerical integration approximation (Equation 4.3.7).

$$\boxed{\int Q^{m_1} \, dt = \sum_{i=0}^{n} \left[\left(\frac{Q_i^{m_1} + Q_{i-1}^{m_1}}{2} \right) \times \left(t_i - t_{i-1} \right) \right]} \qquad (4.3.7)$$

where

t_i = Time at the current time step 'i', (s), and

$Q_i^{m_1}$ = Discharge to the exponent m_1 at the current time step 'i', ($(L/s)^{m_1}$).

The total sediment loss 'T', (g), from the total sediment loss model, comprised both suspended and bedload sediment. The determination of the total suspended sediment loss, (g), for the entire event, '$\int Q_s\, dt$', involved the numerical integration of the suspended sediment discharge (Equation 4.3.8).

$$\boxed{\int Q_s\, dt = \sum_{i=0}^{n}\left[\left(\frac{Q_{s_i} + Q_{s_{i-1}}}{2}\right)\times\left(t_i - t_{i-1}\right)\right]} \qquad (4.3.8)$$

where

Q_{s_i} = Sediment discharge at the current time step 'i', (g/s).

Table 4.3.2 lists the total runoff, (L), and total suspended and bedload sediment loss ,(g), for all events listed in Table 4.3.1.

Table 4.3.2: Eight observed storm events from the natural site and their respective total runoff, (L), total suspended and bedload sediment, (g).

Storm Event.	*Total Runoff, (L).*	*Total Suspended Sediment Loss, (g).*	*Total Bedload Sediment Loss, (g).*	*Total Sediment Loss, (g).*
1197	29445.7	3699.6	3367.8	7067.3
12197	47.1	12.9	771.1	784.0
12197pm	984.3	61.1	65.3	126.4
17197	434.4	224.2	302.7	526.9
211971[st]	258.3	81.1	430.4	511.4
211972[nd]	2867.2	229.2	172.3	401.5
23197	16843.8	1621.0	1145.5	2766.5
28197	5178.1	352.9	368.5	721.5

It can be observed from Table 4.3.2, that the total runoff, (L), from the first storm event occurring on the 12th January of 47.1L, is three orders of magnitude smaller than the total runoff from the storm event occurring on the 1st January. The storm events occurring on the 17th January and the first event on the 21st January, have comparable small total runoff magnitudes to the first event on the 12th January, 434.4 and 258.3 L, respectively. These three storm events were not fitted to the total sediment loss equation because of their small quantity of total runoff compared to the other storm events listed in Table 4.3.2.

Equation (4.3.6) was fitted by regression analysis and the results are illustrated in Figure 4.3.3.

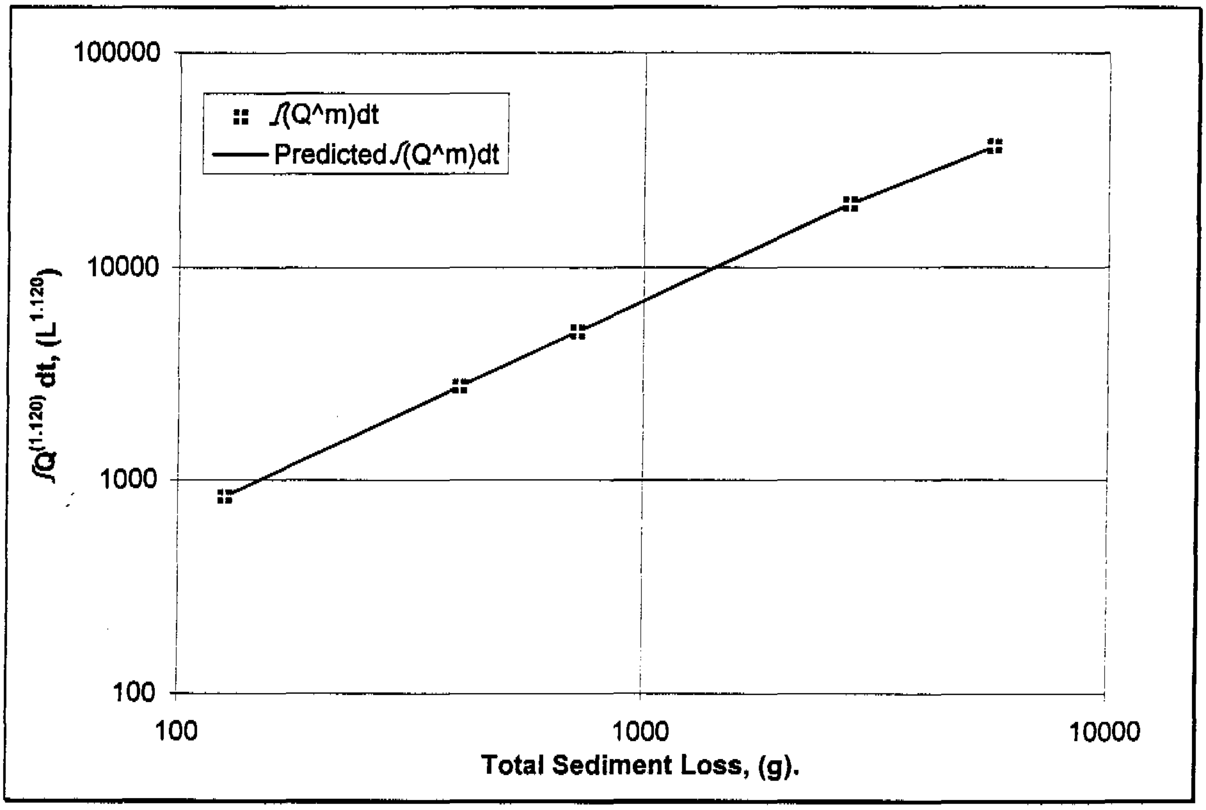

Figure 4.3.3: A log-log regression analysis of the integration of Q^{m1} dt, (L^{m1}), against the total sediment loss, 'T', (g), was performed utilising the five storm events listed in Table 4.3.2.

Equation (4.3.9), highlights the parameter values obtained from the fitting of the total sediment loss model.

$$\boxed{T = 1.171\, W^{(1 - 1.120)} S^{0.69} \int Q^{1.120} dt} \quad (r^2=0.99, df=4, p<0.001) \quad (4.3.9)$$

It can be observed from Equation (4.3.9), that the parameters β_1 and m_1, have mean and standard errors of 1.171 +/- 0.05, and 1.120, respectively. The exponent on the slope term, 'n_1' was assumed to have a magnitude of 0.69, which was similarly adopted for the fitting of the overland flow erosion model. The output from the regression analysis is listed in Appendix 4.C.

4.4 Parameter Comparison

The two sets of erosion parameters, β_1 and m_1, derived from the overland flow erosion model (Equation 4.3.4), and the total sediment loss model (Equation 4.3.9), that were fitted from experimental data from the natural site, are of comparable magnitude (Table 4.4.1).

Table 4.4.1: Comparison between the fitted erosion parameters β_1 and m_1, from the overland flow erosion and the total sediment loss model.

Parameter	***Overland Flow Erosion Model***	***Total Sediment Loss Model***
β_1	0.917	1.171
m_1	0.854	1.120

A comparison between the parameter values obtained from the overland flow erosion model, from the Tin Camp Creek study (Moliere *et al*, 1996), and the current study was necessitated because of insufficient data from the Tin Camp Creek study. Willgoose and Riley (1993) determined erosion parameters from the overland flow erosion model in their study at ERARM, for landform evolution modelling with the program SIBERIA. Table 4.4.2 lists the magnitudes of the β_1 and m_1 parameters obtained from the two studies.

Table 4.4.2: Comparison between the fitted erosion parameters β_1 and m_1, from the overland flow erosion model for the Tin Camp Creek, utilising the complete data set, and data with discharge values less than 10L/s, and the natural site study.

Parameter	***Tin Camp Creek***[a]		***Natural Site***
	Complete Data Set	Data set, Q <10 L/s	
β_1	0.626	0.410	0.917
m_1	1.480	1.371	0.854

[a] Moliere *et al* (1996).

Moliere *et al* (1996) reported that an erosion threshold at approximately 10L/s, appeared to exist in the suspended sediment data set from the Tin Camp Creek study.

It can be observed from Table 4.4.2 that there is considerable difference between the magnitude of the m_1 parameter (the exponent on discharge in Equation 4.2.1), between the Tin Camp Creek Site and the natural site.

A comparison between the parameter values obtained from the total sediment loss model from the current study and previous work from the Northern Waste Rock Dump (Saynor *et al*, 1995), and in the Tin Camp Creek (Moliere *et al*, 1996) is summarised in Table 4.4.3.

Table 4.4.3: Comparison between the fitted erosion parameters β_1 and m_1, from the total sediment loss model for studies conducted on the Northern Waste Rock Dump, in the Tin Camp Creek area, and the current study.

Parameter	***Northern Waste Rock Dump*** [a]			***Tin Camp Creek***	***Natural Site***
	Cap Site	Batter Site	Soil Site	Mica and Quartz Site [b]	
β_1	12.76	3.08	23.29	2.86	1.171
m_1	1.67	1.67	1.67	1.33	1.120

[a] Saynor *et al* (1995)
[b] Moliere *et al* (1996), n_1= 1.19

The parameters reported in Table 4.4.3 for Northern Waste Rock Dump (Saynor *et al*, 1995), are from data sets collected in 1993 (cap and batter sites) and in 1995 (soil site). In all cases the 'n_1' exponent on the slope term of the total sediment loss model was fixed at a constant 0.71 (Equations 4.4.1 to 4.4.3).

$$\boxed{T(cap) = 12.76\ W^{(-0.67)} S^{0.71} \int Q^{1.67} dt} \quad (r^2 = 0.90, df=30) \quad (4.4.1)$$

$$\boxed{T(batter) = 3.08\ W^{(-0.67)} S^{0.71} \int Q^{1.67} dt} \quad (r^2 = 0.90, df=30) \quad (4.4.2)$$

$$\boxed{T(soil) = 23.29\ W^{(-0.67)} S^{0.71} \int Q^{1.67} dt} \quad (r^2 = 0.90, df=30) \quad (4.4.3)$$

Due to data shortages in the Tin Camp Creek study, a modification of the total sediment loss model (Equation 4.4.4), was fitted to the experimental data (Moliere *et al,* 1996).

$$\boxed{\frac{T}{S^{n_1}} = \beta_1 \int Q^{m_1} dt} \qquad (4.4.4)$$

The results listed in Table 4.4.3, for the Mica and Quartz sites are derived from Equation (4.4.5), with the 'n_1' exponent, fixed at a constant 1.19.

$$\boxed{\frac{T}{S^{1.19\pm0.03}} = 2.857^{+0.91}_{-0.69} \int Q^{1.33\pm0.503} dt} \qquad (4.4.5)$$

The constant 'n_1' term was derived from regression analysis of suspended sediment concentration reported in Moliere *et al* (1996).

The two erosion models in this study, utilised different data sets; suspended sediment for the overland flow erosion model; and bedload and suspended sediment for the total sediment loss model. The two models independently achieved erosion parameter values for β_1 and m_1, that were similar in magnitude. A comparison between the results from the Tin Camp Creek and the current study (Table 4.4.2), highlighted that a general trend existed, that is the rate of sediment transport is predicted to be higher in the Tin Camp Creek area than on the natural site. This comparison is based on the values for the parameter m_1, which is the exponent of Equation (4.2.1). This exponent on discharge, tends to govern the overland flow erosion model.

Table 4.4.3 highlights a more conclusive trend with respect to the erosion pararameter values derived from the total sediment loss model for the NWRD, Tin Camp Creek and the current study. As previously reported (Section 1.0), the NWRD is considered to represent the weathered state of waste rock material after 10 years of exposure, the Tin Camp Creek site is assumed to represent waste rock material after at least 100 years of exposure. Finally the current study is assumed to represent waste rock material after at least 100,000 years of exposure. The natural site had the lowest magnitude of β_1 and m_1, of 1.170 and 1.120, respectively, which implies that the sediment transportation rate is lowest for the current study. The β_1 and m_1 values from the Tin Camp Creek study were in between the results obtained from the current study and those obtained from studies on the NWRD, suggesting that the assumption that the Tin Camp Creek site represents medianly weathered waste rock material is not inconsistent with the data.

The exponent m_1, from the cap, batter and soil sites from the NWRD, were of similar magnitudes but noticeably higher than those values reported for the other studies. The β_1 parameter values from the NWRD were consistently higher than those values reported from other studies, except for the batter site where the value of 3.08 obtained is only marginally higher than the value of 2.86, from the Tin Camp Creek study.

5.0 Evaluation of the Effect of Vegetation Growth Over Wet Season

The vegetation present on the field site was non-uniform in both ground cover and leaf surface area. Numerous species of trees and low shrubs were present on the site as well as a large quantity of developing spear grass. The evaluation of vegetation growth throughout the 1996/1997 wet season was not quantified, however Figures 5.1, 5.2, and 5.3, are photographs from the site on the 5th, and 30th December, and the 29th January, and serve to illustrate the development of vegetation, especially spear grass.

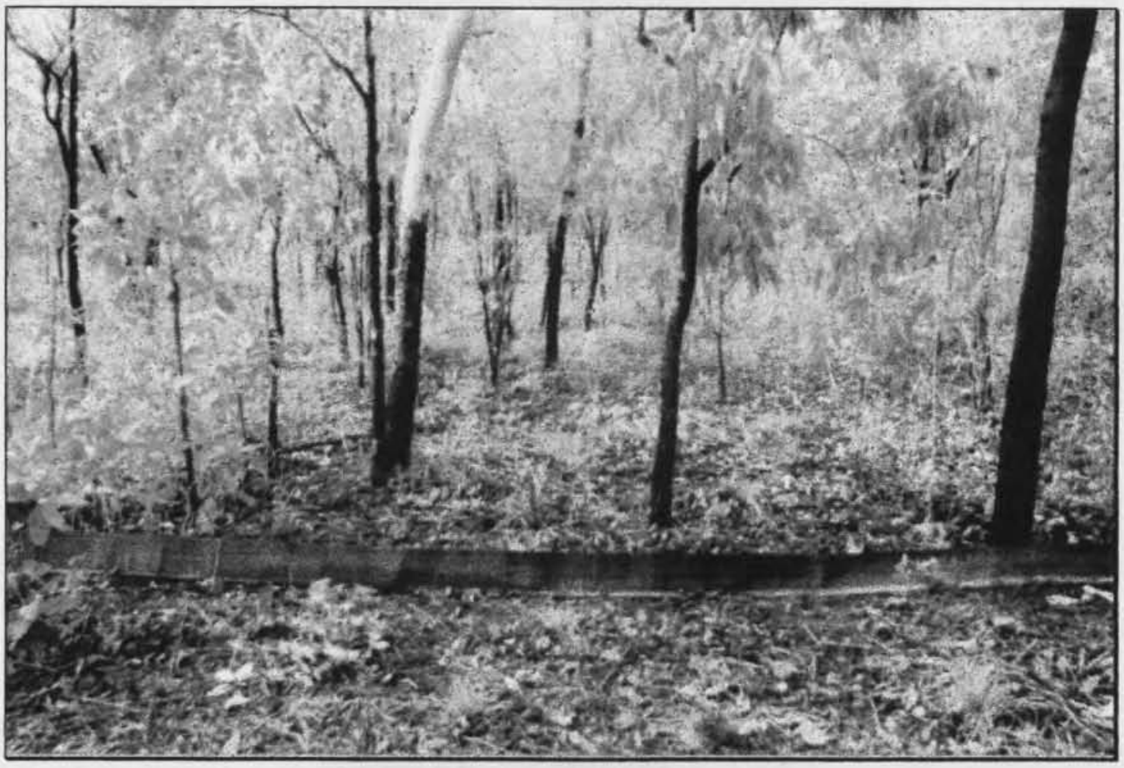

Figure 5.1: Natural field plot, 5th December 1996.

Figure 5.2: Natural field plot, 30th December 1996.

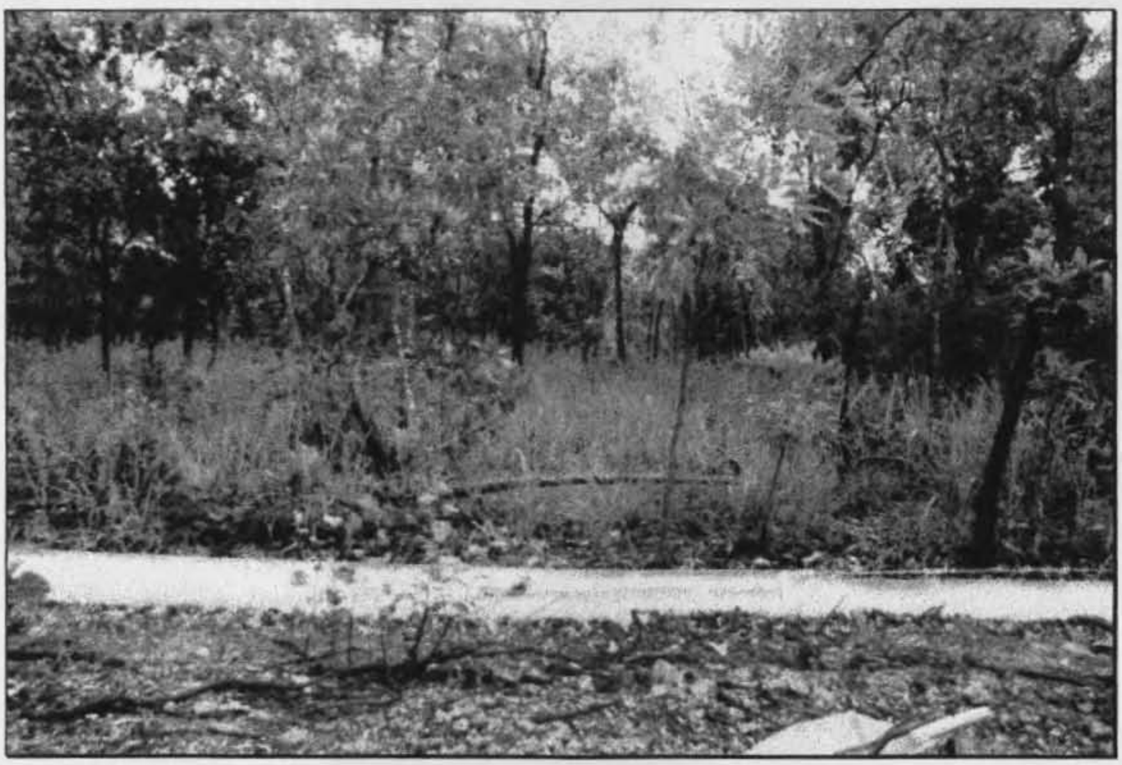

Figure 5.3: Natural field plot, 29th January 1997.

The main trunk and rooting system of the spear grass occupies only a relatively small area at the ground level in comparison to other larger shrub and tree plant species. As the spear grass can grow to considerable height, some metres during the wet season, the change in the leaf interception area of this species was hypothesised to have an effect on the quantity of rainfall hitting the soil.

The large amount of decomposing leaf litter (Figure 5.4), built up over the dry season, provides a shield for the soil underneath.

Figure 5.4: Decomposing leaf litter from the previous wet season slowly breaks down during the course of the year and provides considerable coverage of the soil surface.

The kinetic energy of rainfall impacting the soil will be reduced by this leaf litter. Exposed sections, devoid of leaf litter near the PVC pipe, due to construction were affected by splash erosion. The impact of exposed soil on the transport of sediment during the experiment was considered negligible as the 300 millimetre diameter PVC pipe was completely installed by late November, and monitoring did not commence until late December. The area of soil subjected to increased splash erosion was only a very small fraction of the 600 square metre site.

A considerable degree of storm activity occurred towards the end of February which exhibited different behaviour with respect to kinematic wave parameter values to those storm events that occurred towards the start of the wet season. Table 5.1 is a summary of the kinematic wave and infiltrative loss parameter values from Table 3.7.2, to highlight the differences between events occurring at the start of the wet season and those events occurring at the end of wet season.

Table 5.1: Summary of kinematic wave parameter values for eight storm events from the current study that occurred at the start of January and the end of February.

Storm Event	*Peak Runoff, L/s.*	*Kinematic Wave Parameters*	*Mean (Standard Deviation)*	*Infiltration Parameters*	*Mean (Standard Deviation)*
1/1/97	11.00	C_r	1.684(0.081)	S_ϕ (mm/hr$^{1/2}$)	7.948(1.525)
		e_m	1.675(0.083)	ϕ(mm/hr)	0.280(2.247)
3/1/97	6.00	C_r	4.480(1.574)	S_ϕ (mm/hr$^{1/2}$)	0.245 (1.839)
		e_m	1.544(0.199)	ϕ(mm/hr)	13.64(2.071)
4/1/97	1.30	C_r	0.775 (0.137)	S_ϕ (mm/hr$^{1/2}$)	0.001 (214.54)
		e_m	1.291 (0.108)	ϕ(mm/hr)	3.783 (88.194)
23/1/97	12.00	C_r	2.258 (0.106)	S_ϕ (mm/hr$^{1/2}$)	0.001 (1867.6)
		e_m	1.596 (0.068)	ϕ(mm/hr)	51.58 (246.60)
20/2/97	4.00	C_r	3.211(0.505)	S_ϕ (mm/hr$^{1/2}$)	2.2578(1.913)
		e_m	2.093(0.189)	ϕ(mm/hr)	22.743(4.03)
22/2/97	4.00	C_r	4.336 (0.506)	S_ϕ (mm/hr$^{1/2}$)	0.001 (124.55)
		e_m	2.108 (0.080)	ϕ(mm/hr)	15.541 (3.47)
22/2/97pm	3.70	C_r	11.58 (2.402)	S_ϕ (mm/hr$^{1/2}$)	3.236 (0.689)
		e_m	2.236 (0.135)	ϕ(mm/hr)	0.001 (1.049)
23/2/97	3.30	C_r	6.110 (1.591)	S_ϕ (mm/hr$^{1/2}$)	3.235 (0.689)
		e_m	2.077 (0.246)	ϕ(mm/hr)	0.001 (1.049)

Storm events occurring towards the end of February generally had e_m values noticeably higher than events occurring at the beginning of the wet season. Figure 5.1 illustrates this trend with storm events; 20th, 22nd, 22nd pm, and 23rd of February having a mean e_m value well above storm events; 1st ,3rd , 4th , and the 23rd of January.

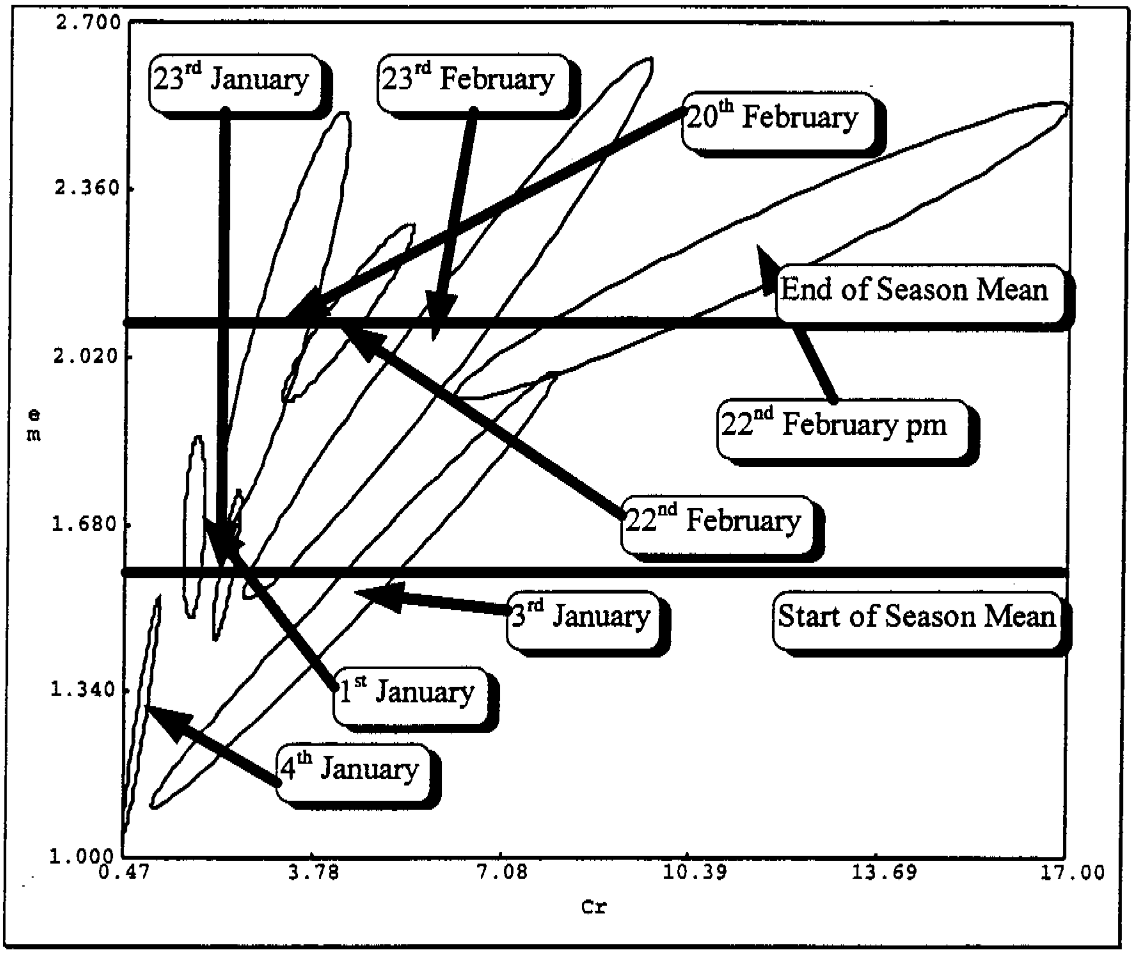

Figure 5.1: 95% posterior probability plot of the kinematic wave parameters C_r and e_m, for the eight storm events listed in Table 5.1. The eight storm events were divided into two groups, those occurring at the start and at the end of the wet season, each with their on defined mean.

The mean e_m value at the start of the wet season, highlighted by the lower large line in Figure 5.1, for the storm events occurring on the 1st ,3rd , 4th , and the 23rd of January, was determined to be 1.53. The mean e_m value at the end of the wet season, highlighted by the upper large line in Figure 5.1, for the storm events occurring on the 20th, 22nd, 22nd pm, and 23rd of February, was determined to be 2.13.

Figure 3.2.5 illustrates four different hillslope geometries that are governed by the exponent of the power law function, e_m. Comparison of the mean e_m values of 1.53 and 2.13 with the e_m values of the different hillslope geometries from Figure 3.2.5, tends to indicate that the hillslope surface became less hydraulically rough throughout the wet season.

The peak recorded discharges for eight storm events (Table 5.1), were fairly uniform, hence the possible influence of differences between discharge peaks was ignored.

As the wet season progressed, more of the hillslope was behaving as constant depth sheet flow (Geometry A, Figure 3.2.5), which may be a function of the saturated hydraulic conductivity of the soil. It is hypothesised that no major changes in the hillslope cross sectional area occurred during the course of the wet season as a result of erosion.

A plot of the values of sorptivity over the wet season from Table 5.1, does not highlight any conclusive trends.

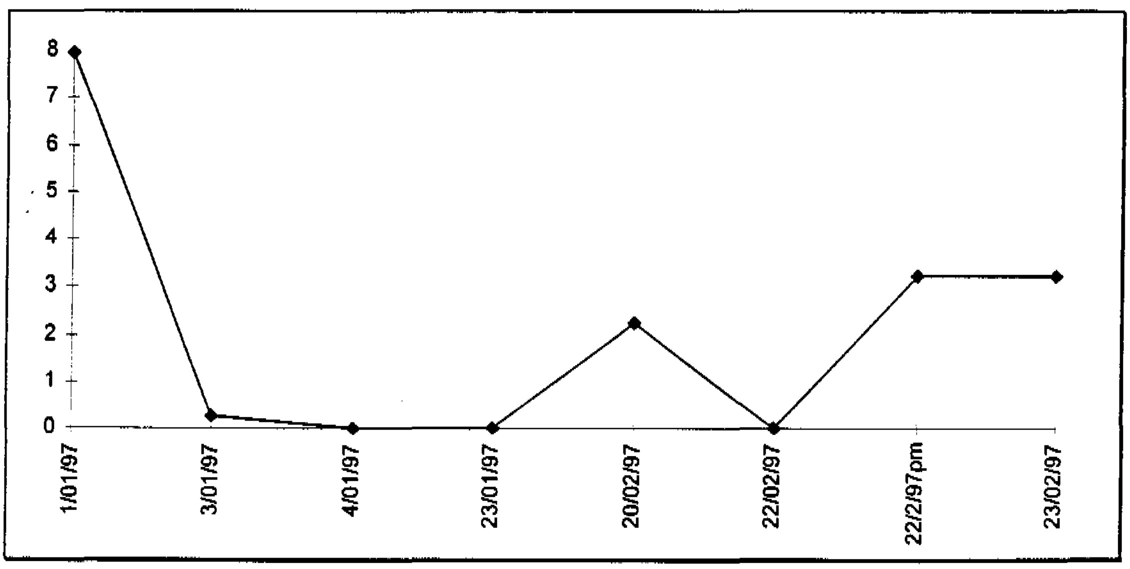

Figure 5.2: Plot of the S_ϕ values fitted from DISTFW-NLFIT, for eight storm events that occurred over the wet season that are listed in Table 5.1.

A similar plot of the values of the continuing loss parameter, ϕ, for the eight storm events listed in Table 5.1, does reflect a possible trend.

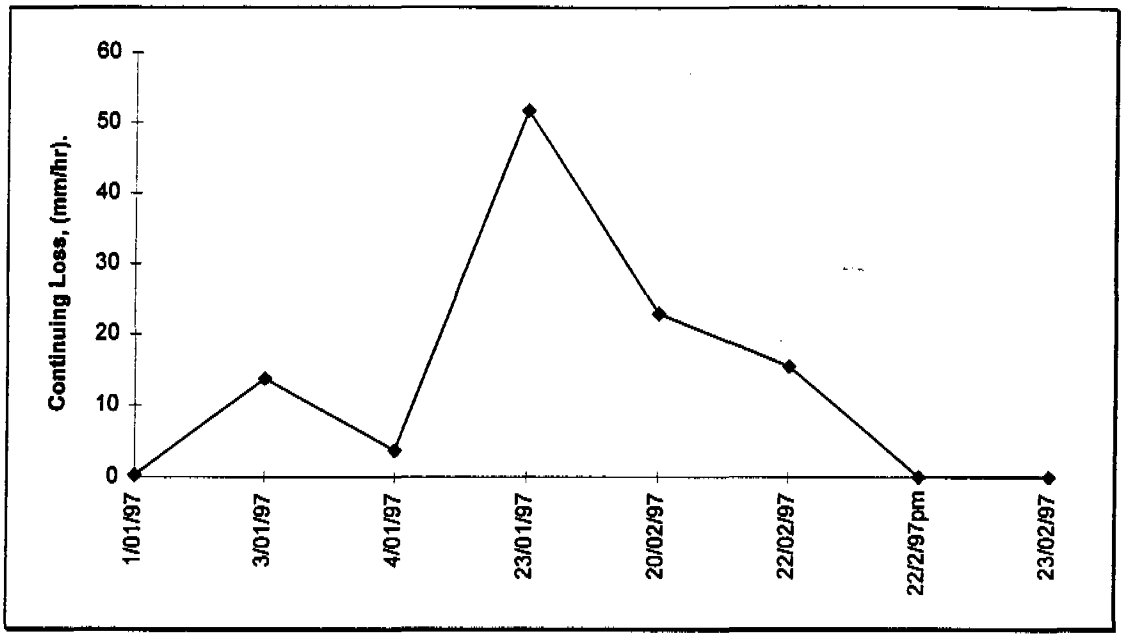

Figure 5.3: Plot of the ϕ values fitted from DISTFW-NLFIT, for eight storm events that occurred over the wet season that are listed in Table 5.1.

The storm event that occurred on the 4th January had a small peak discharge (1.3 L/s), when compared to 6 and 12 L/s for storm events occurring on the 3rd and 23rd January, respectively. By the omission of the 4th January storm event, a trend of increasing then decreasing continuing loss rates throughout the wet season is evident.

It is hypothesised that the effect of leaf interception area would not be as great as the effect of the withdrawal of water from the upper portions of the soil matrix by the extremely fast growing spear grass and other vegetation. Due to the distinct short wet season, it is believed that the vegetation would have a tendency to increase water uptake during this period due to water availability. Increased and then decreased water removal couple with the previously hypothesised decrease in hydraulic conductivity of the soil matrix over the wet season due to saturation goes a part of the way to attempt to explain the behaviour of the plot of continuing loss against time (Figure 5.3)

6.0 Further Work

Further natural storm event monitoring on the field for the purpose of sediment transportation parameter estimation is not considered by the author as necessary because of the significant results obtained and reported.

For reasons stated previously, one set of DISTFW parameters could not be fitted to a number of combinations of four storm events, similar to that conducted in the Tin Camp Creek study. Although this limitation was overcome, multiple storm event calibration should be theoretically possible and may warrant further investigation for confirmation of results.

A brief evaluation of the possible effect of vegetation growth over the wet season on the field plot was conducted, however, further work needs to be conducted to quantify the hydrologic effect of this growth. Two small natural field plots could be constructed and monitored during the wet season, with one acting as the control, by allowing vegetation to grow (especially spear grass), and one where the spear grass was carefully removed.